AIAA Atmospheric Flight Mechanics Conference and Exhibit
15 - 18 August 2005, San Francisco, California

AIAA 2005-6229

A First-Order, Simplified, Conservative Methodology for Computing Reentry Casualty Expectation

Jeffrey Tooley*
The Aerospace Corporation, El Segundo, CA, 90291

Trent Habiger† and K. Rolf Bohman‡
The Aerospace Corporation, El Segundo, CA, 90291

Lyndon Bonaparte§
Federal Aviation Administration, Washington, DC, 20591

Casualty expectation is a measure of risk associated with the overflight of populated areas during the launch and reentry of space vehicles. Numerous methodologies exist for computing casualty expectation throughout the government and industry. These methodologies incorporate models for calculating failure conditions, debris impact areas, debris impact characteristics, and the population at risk. As a result of the recent Space Shuttle *Columbia* failure, computing casualty expectation for reentry from low Earth orbit has been at the forefront of the range safety community. Due to the high aero-thermal loads experienced during reentry, computing casualty expectation requires additional modeling consideration than what is required for a similar analysis during launch. These additional considerations include modeling the structural breakup of the spacecraft due to aero-thermal effects and modeling the large, complicated debris impact areas affected by atmospheric drag and other perturbations. This paper presents first-order, simplified, conservative models that are combined to create a casualty expectation computation methodology that can be used for reentry mission planning. In this methodology casualty expectation is expressed in terms of its key elements: the vehicle failure conditions, the resulting debris casualty area, the probability of the debris impacting a certain area, and the population at risk. The failure state is computed along the vehicle's nominal trajectory and the resulting discrete breakup points are fed into the debris breakup, casualty area, debris survivability, and impact probability models. The Model for computing the casualty area includes a simple debris breakup model, as well as simple equations for computing aerodynamic properties based on the debris shape. A model, which utilizes debris survivability lookup tables, has also been provided for determining whether debris survives. A model that combines a time-based estimate of the failure probability with a uniform downrange and normal crossrange impact probability density function is used to determine the debris impact probability. The population model is based on a world centroidal population database coupled with a kinetic energy sheltering factor. These models are combined to form a comprehensive methodology for computing the total casualty expectation for reentry.

Nomenclature

A_p	=	projected area
A_{sc}	=	sheltered casualty area
A_{tsc}	=	total sheltered casualty area

---

* Sr. Member of the Technical Staff, Flight Mechanics Department at The Aerospace Corporation. Currently employed by the Jet Propulsion Laboratory.
† Member of the Technical Staff, Flight Mechanics Department.
‡ Section Manager, Flight Mechanics Department.
§ Aerospace Engineer, Office of Commercial Space Transportation.

Copyright © 2005 by the American Institute of Aeronautics and Astronautics, Inc.
The U.S. Government has a royalty-free license to exercise all rights under the copyright claimed herein for Governmental purposes.
All other rights are reserved by the copyright owner.

A_{uc}	=	unsheltered casualty area
A_w	=	wetted area
C_{Dhc}	=	hypersonic continuum drag coefficient
C_{Dsub}	=	subsonic continuum drag coefficient
cr	=	crossrange
cr_A	=	crossrange distance to center of population centroid
d	=	debris subscript
DR	=	downrange length of debris line
dr	=	downrange
dt	=	debris wall thickness
E_c	=	casualty expectation
$f(dr,cr)$	=	probability density function
F_{ps}	=	fraction of people under s^{th} shelter type
h	=	height also used as altitude at breakup in survivability tables
i	=	breakup point subscript
I_f	=	impact factor
j	=	area subscript
KE	=	kinetic energy
l	=	length
l_c	=	equivalent cylinder length
p	=	phase of flight subscript
P	=	population count
P_{cs}	=	probability of casualty for s^{th} shelter type
PD	=	population density
P_f	=	probability of failure
PI	=	probability of impact
r	=	radius
r_c	=	equivalent cylinder radius
r_h	=	heating radius
r_i	=	inner radius
r_n	=	new radius after melting
r_p	=	radius of a person
s	=	sheltering type subscript
S	=	aerodynamic reference area
t	=	trajectory time
T	=	Temperature at breakup
v	=	Earth relative velocity at breakup
w	=	width
W	=	debris weight
W_n	=	new weight after melting
β_{hc}	=	hypersonic continuum ballistic coefficient
β_{sub}	=	subsonic continuum ballistic coefficient
γ	=	geocentric Earth relative flight path angle
Δcr	=	crossrange length of population area
Δdr	=	downrange length of population area
Δt	=	dwell time
ρ_{mat}	=	material density
ρ_{sl}	=	air density at sea level
σ_{cr}	=	crossrange standard deviation

I. Introduction

THE goal of this paper is to develop first-order, simplified models that can be used for mission planning to compute casualty expectation during the high heating phase of low Earth orbit reentry flight. Casualty expectation is a measure of risk to people on the ground associated with the overflight of populated areas by a

launch or reentry space vehicle. Currently within industry and government there are numerous methodologies for computing casualty expectation. These methodologies incorporate models for calculating failure conditions, debris impact areas, debris impact characteristics, and the population at risk. Due to many factors such as the type of mission, vehicle, and modeling requirements, these models are of varying fidelity, complexity, and conservatism. For example, models range from a simple tabular lookup of random reentry impact probability based on the spacecraft orbital inclination[1], to a higher fidelity debris survivability tool for computing casualty area for reentry[2], to a rigorous Monte Carlo analysis used to compute the debris area impact probability.

Since the release of the *Columbia Accident Investigation Board Report*[3], developing methodologies for computing casualty expectation for reentry from low Earth orbit has been at the forefront of the range safety community. Reentry has unique requirements for computing casualty expectation, therefore new models need to be developed that will address some of the issues specific to reentry. Particular issues include reentry failures involving large debris impact areas, vehicle breakups that include aero-thermal effects, and impact locations that must be represented by modeling a large and diverse group of debris falling to the ground.

The casualty expectation methodology developed in this paper can be broken into the computation of four parts: the breakup points, the debris casualty area, the debris impact probability, and the population at risk. Section II addresses how to choose the breakup point failure states given a nominal reentry. These breakup point states become inputs for the other parts of the casualty expectation methodology listed above. Section III demonstrates how to compute casualty area. This computation requires the development of a simple debris model, computation of aerodynamic properties based on debris shape, the development of a population sheltering model, and the use of debris survivability lookup tables. Section IV describes the calculation of debris impact probability. This calculation is based on modeling the vehicle's failure probability and generating an impact probability density function using a uniform downrange distribution and a normal crossrange distribution. Section V describes how to access and use a centroidal population database. Section VI describes how each of these models is combined to compute a total casualty expectation.

II. Establishing Breakup Point State

The first step in establishing overflight risk due to a planned reentry is to establish a mission-specific trajectory. Typical trajectory state information required for this computation includes: a discrete trajectory timeline, altitude, velocity, flight path angle, flight azimuth, longitude, and latitude. To help with visualizing some of the concepts introduced in this paper, an example trajectory of a wing-body reentry from low Earth orbit will be used. The ground trace for this trajectory is shown in Figure 1.

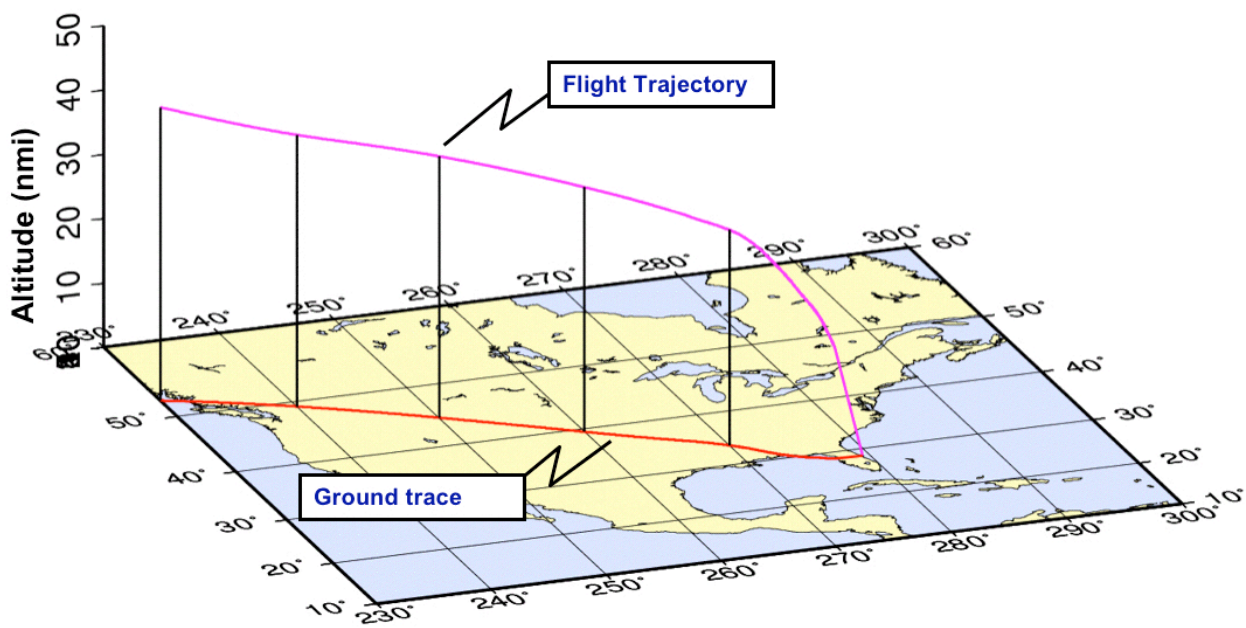

Figure 1. Illustration of Wing-Body Reentry Trajectory.

As was stated in the Section I of this paper, this methodology focuses on the high heating portion of reentry. Based on experience, most spacecraft reentering from low Earth orbit will encounter their highest thermal loading

between 46 to 30 nmi altitude[4]. This phase of flight, referred to as the high heating phase, will be the focus of this methodology.

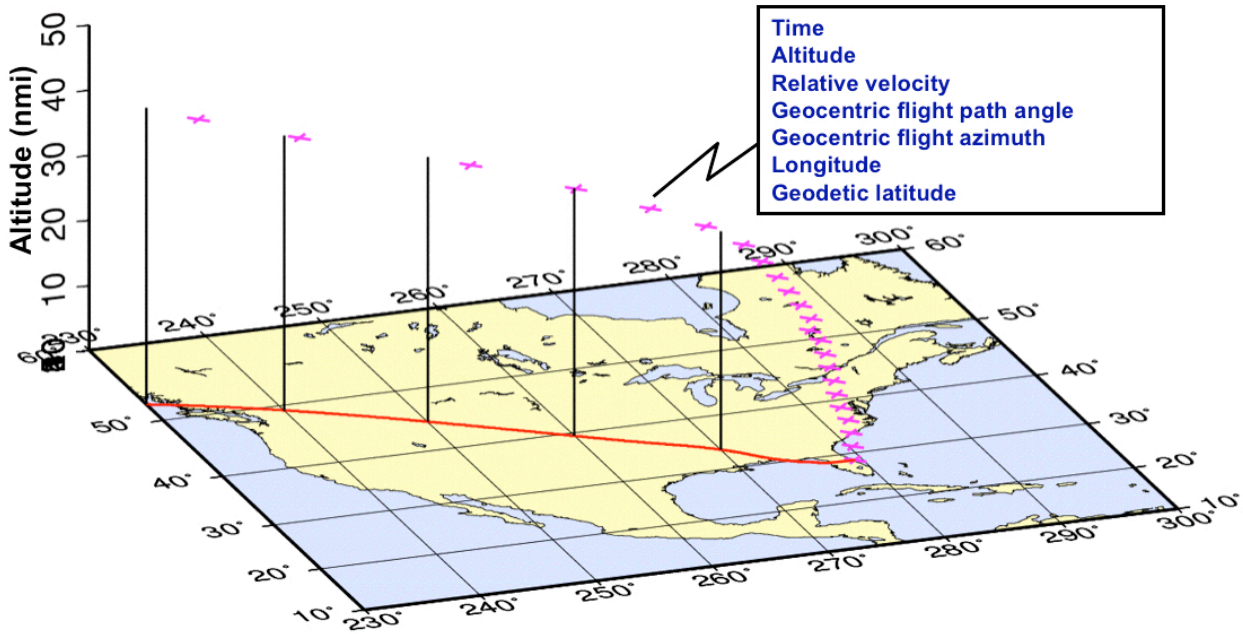

Figure 2. Illustration of Discretized Breakup States.

The nominal trajectory during the chosen phase of flight is discretized to represent possible breakup points. A casualty expectation value will be computed for each of these breakup points. Based on experience, spacing the discrete steps at an altitude change of every 2 nmi should be adequate for a first-order approximation. Figure 2 shows an example of a discretized trajectory with breakup points plotted every 2 nmi.

III. Determining Debris Model, Casualty Area, and Debris Survivability

Casualty area is a representation of the area in which people are at risk from a piece of falling debris impacting the ground. The models described in this section form the basis for computing a total sheltered casualty area. These models incorporate a method for characterizing the debris after breakup, a method for computing the casualty area and aerodynamic properties based on the shape of the debris, a method for determining the aero-thermal debris survivability based on lookup tables, and a population sheltering model.

A. Debris Breakup Model

The breakup points shown in Figure 2 can result from aerothermal heating, aerodynamic forces, explosion, or other failure modes. Because low Earth orbit reentry involves high velocities and high temperatures, it is assumed that there is an instantaneous separation of all major structural components as the result of aerodynamic forces and heating. This includes boxes, tanks, engines, batteries, pieces of structure, solar panels, etc. This is a simplification of the breakup of the spacecraft because it assumes primary breakup only. In reality, most aerothermal breakups involve primary, secondary, and many more breakups. To ensure that this method remains conservative in light of this simplification, it is important to note that the more pieces of debris that are created, the larger the casualty area. Therefore, when uncertain whether a piece of debris will break apart from a larger chunk, assume it does. The characteristics of the debris that should be noted in the debris model are shape, material, size, and weight of the debris.

A special note is made about survivability here. If survivability is part of a breakup analysis, assuming debris instantly separates can result in a smaller, less conservative casualty area. This is because secondary breakups can shield debris from heating and can increase debris survivability. This effect is countered by conservatively choosing the debris temperature at breakup for the debris survivability analysis described in Section IIID.

B. Debris Aerodynamic Properties and Unsheltered Casualty Area

Once a debris model is created, Table 1 provides equations for determining the aerodynamic properties and the unsheltered casualty area of the debris based on its shape, size, and weight. There are four shapes available in this table: tumbling hollow sphere, tumbling hollow cylinder, tumbling flat plate, and tumbling hollow box. *Tumbling* implies that the aerodynamic properties were generated for a tumbling rather than trimmed debris. *Hollow* means that the mass is distributed along the walls of the debris in a shell shape. If an approximate shape cannot be found in these tables, other methods should be used to determine the unsheltered casualty area and aerodynamic properties.

Some of the calculations shown in this table are also used to compute the debris survivability and impact probability density function. The inputs required to determine the aerodynamic properties and the unsheltered casualty area are listed below each shape name along with the geometry constraints for which these equations apply.

Table 1. Shape Based Equations for Aerodynamic Properties and Unsheltered Casualty Area

Shape	Tumbling hollow sphere	Tumbling hollow cylinder	Tumbling flat plate	Tumbling hollow box
Shape variables with geometry constraints	weight (W) radius (r)	weight (W) radius (r) length (l) $l > 2r$	weight (W) length (l) width (w) $l > w$	weight (W) length (l) width (w) height (h) $l > w > h$
Wetted area (A_w)	$4\pi r^2$	$2\pi r(r+l)$	$2lw + 2lt + 2wt$	$2\pi r_c(r_c+h_c)$
Hypersonic continuum drag coefficient (C_{Dhc})	0.92	$0.720 + 0.326(2r/l)$ [Ref. 5]	1.84	$0.720 + 0.326(2r_c/l_c)$
Subsonic drag coefficient (C_{Dsub})	0.48	$0.360 + 0.326(r/l)$	0.92	$0.360 + 0.326(r_c/l_c)$
Aerodynamic reference area (S)	πr^2	$2rl$	lw	$2r_ch_c$
Hypersonic continuum ballistic coefficient (β_{hc})	$W/S/C_{Dhc}$	$W/S/ C_{Dhc}$	$W/S/ C_{Dhc}$	$W/S/ C_{Dhc}$
Subsonic ballistic coefficient (β_{sub})	$W/S/ C_{Dsub}$	$W/S/ C_{Dsub}$	$W/S/ C_{Dsub}$	$W/S/ C_{Dsub}$
Heating radius (r_h)	r	r	w/2	r_c
Projected Area (A_p)	$\pi r2$	Whichever is greater: $2rl$ or $\pi r2$	lw	lw
Unsheltered casualty area (A_{uc}) with man border (r_p = 1 ft)	$\pi(r+r_p)^2$	Whichever is greater: $2(r_p+r)(l+2r_p)$ or $\pi(r+r_p)^2$	$(l+2r_p)(w+2r_p)$	$(l+2r_p)(w+2r_p)$
Terminal kinetic energy (KE) at sea level with air density (ρ_{sl})	$W\beta_{sub}\rho_{sl}$	$W\beta_{sub}\rho_{sl}$	$W\beta_{sub}\rho_{sl}$	$W\beta_{sub}\rho_{sl}$
Equivalent cylinder length (l_c)	n/a	n/a	n/a	l
Equivalent cylinder radius (r_c)	n/a	n/a	n/a	$\sqrt{((wh)/\pi)}$
Wall thickness (dt) with material density (ρ_{mat})	n/a	n/a	$W/\rho_{mat}/l/w$	n/a

C. Sheltered Casualty Area

Once the unsheltered casualty area is computed from Table 1, the sheltered casualty area is calculated from

$$A_{sc} = I_f A_{uc} (P_{c1} F_{p1} + P_{c2} F_{p2} + P_{c3} F_{p3}) . \quad (1)$$

The impact factor (I_f) in Eq. (1) is used to represent debris impact characteristics such as splatter, skid, bounce, ricochet, and cratering effects[6]. For conservatism a value of 2 is chosen for this impact factor (I_f). This value is considered conservative because most reentries involve debris that will be falling vertically when it hits the ground and will not necessarily skid or ricochet. This impact factor (I_f) of 2 does not account for the debris exploding upon impact; if the debris is explosive, other factors must be applied[7]. Eq. (1) also includes the effect of sheltering based on Table 2. Table 2 bases the probability of casualty for the sth type of sheltering (P_{cs}) on the debris kinetic energy (KE) at impact, and combines this with the fraction of people under each sth type of sheltering (F_{ps}). As long as the sum of the fractions equals one and justification is given, the fractions under each type of sheltering can be reshuffled based on overflight of different geographical regions or during different times of day.

Table 2. Sheltering Parameters for Eq. (1)

Shelter Type	Description	Kinetic energy (KE) based probability of casualty (P_{cs}) for the sth shelter type	Fraction of people under specified s^{th} shelter (F_{ps})

1	Building with concrete or reinforced roof	If (KE > 74000 ft-lb); $P_{c1} = 1$
		If (6200 ft-lb ≤ KE ≤ 74000 ft-lb); P_{c1} ramps linearly from 0 to 1
		If (KE < 6200 ft-lb); $P_{c1} = 0$
			$F_{p1} = 0.2$

2	Single story building such as houses or trailers	If (KE > 3200 ft-lb); $P_{c2} = 1$
		If (100 ft-lb ≤ KE ≤ 3200 ft-lb); P_{c2} ramps linearly from 0 to 1
		If (KE < 100 ft-lb); $P_{c2} = 0$
			$F_{p2} = 0.7$

3	Unsheltered	If (KE > 35 ft-lb); $P_{c3} = 1$ If (0 ≤ KE ≤ 35 ft-lb); P_{c3} ramps linearly from 0 to 1	$F_{p3} = 0.1$

D. Debris Survivability

Due to the high atmospheric heating associated with low Earth orbit reentries, the possibility exists for the debris to melt before it hits the ground. A method has been developed to determine debris survivability based on tabular lookups. The method is a first-order analysis; if a more detailed analysis is needed the user should use a higher fidelity tool such as ORSAT[2]. The debris survivability lookup tables are generated by parametrically varying the debris breakup state and geometry. The resulting thousands of cases are then run in a simplified heating analysis tool to determine debris survivability. The heating analysis tool is based on integrating the Detra-Kemp-Riddell heating equations[8] for a trajectory propagated forward from the breakup state. In order to reduce the number of variables being parametrically varied and the run time of each case, the assumptions in Table 3 are made.

Table 3. Debris Survivability Table Assumptions

- Survivability is weakly dependent on breakup flight azimuth, breakup latitude, and breakup longitude, therefore, these variables are set to 90˚, 0˚, and 0˚, respectively
- A stagnation heating area averaging factor of 0.12 is used, this factor is applied to the Detra-Kemp-Riddell stagnation heat rate
- The atmosphere used for reentry is the 1962 United States Standard Atmosphere
- Hypersonic continuum ballistic coefficient from Table 1 is used for aerodynamic property modeling
- A heating radius in accordance with Table 1 is used
- Shape and mass properties are assumed to be constant throughout melting
- The heating calculations treat the spacecraft as a lump mass, and no spatial gridding is done; the temperature of the lump changes in time with the total heat content
- There are no secondary breakups; the debris begins falling on its individual trajectory from the moment the breakup state is reached
- Material properties in accordance with Table 4 are used

Table 4. Debris material properties[9]

Material	Melt temperature (°R)	Specific heat capacity (BTU/lb/°R)	Heat of fusion (BTU/lb)	Material density (lb/ft^3)
Aluminum 2024-T8xx	1541	0.232	166	175
Titanium (6 Al-4 V)	3497	0.192	169	277
Stainless Steel 21-6-9	3110	0.105	123	489

Based on these assumptions debris survivability is reduced to a function of debris shape, debris material, debris geometry, debris temperature at breakup, debris velocity at breakup, debris altitude at breakup, and debris flight path angle at breakup. Debris survivability in the tables is represented by the liquid fraction (LF), which is a measure of the fraction of debris that has melted. The liquid fraction is computed by the simplified heating analysis described above. A liquid fraction of 1 means all debris has melted and a 0 means no debris has melted. The legend used for the debris survivability tables for spherical debris is shown in Table 5. Because the tables take up a large amount of space, only a small set of six debris survivability tables are shown in Figs. 3a-f for spherical debris.

The tables are used by looking up the liquid fraction based on the discrete breakup state and the debris geometry parameters listed in Table 5. Figs. 3a-b show that all of the titanium and stainless steel debris survives even for high breakup temperatures and velocities. The aluminum debris survivability in Figs. 3c-f show that, in general, debris survivability increases as both mass and radius of the sphere increase. Survivability for aluminum sphere debris is shown for two debris temperatures at breakup (540°R and 1541°R). The conservative solution of 540°R should be used unless it is known that a material will be exposed to the freestream air until breakup.

Based on the liquid fraction (LF), the original sphere weight (W), the original sphere radius (r), and material density (ρ_{mat}), the new weight (W_n), and new radius (r_n) of a hollow sphere after melting are computed using Eqs. 2-5. This new debris geometry is calculated according to the melt direction and the resulting shape parameters are fed into Table 1 to compute the surviving unsheltered casualty area. For these equations it is assumed that the mass of the sphere is distributed along the wall and the melt direction is along the thickness of the sphere.

$$W_n = W(1 - LF) \tag{2}$$

$$r_n = \frac{1}{2\rho_{mat}\pi}\left(\rho_{mat}{}^2\pi^2\left(6W + 8r_i^3\rho_{mat}\pi\right)^{1/3}\right) \tag{3}$$

where the sphere inner radius (r_i) is defined as:

$$r_i = r - dt \tag{4}$$

and the initial debris wall thickness (dt) is:

$$dt = \frac{1}{2\rho_{mat}\pi}\left(\rho_{mat}{}^2\pi^2\left(6W - 8r^3\rho_{mat}\pi\right)^{1/3}\right) + r\,. \tag{5}$$

A set of similar equations can be employed to calculate the melted parameters for other shapes in the debris model.

Table 5. Debris Survivability Legend for Spherical Debris

Survivability table lookup variables
T – temperature at breakup (°R)
h – altitude at breakup (nmi)
v – Earth relative velocity at breakup (ft/s)
γ – Earth relative geocentric flight path angle at breakup (deg)
W – weight at breakup (lb)
r – sphere outside wall radius at breakup (ft)

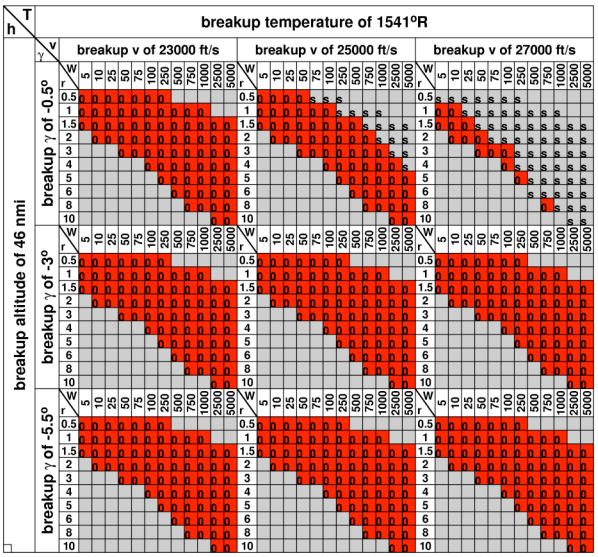

Figure 3a. Stainless Steel Tumbling Hollow Sphere Survivability for Breakup Altitude of 46 nmi and Breakup Temperature of 1541°R

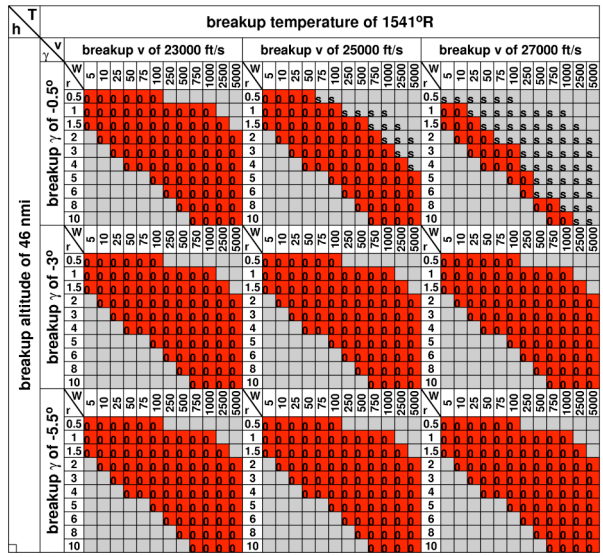

Figure 3b. Titanium Tumbling Hollow Sphere Survivability for Breakup Altitude of 46 nmi and Breakup Temperature of 1541°R

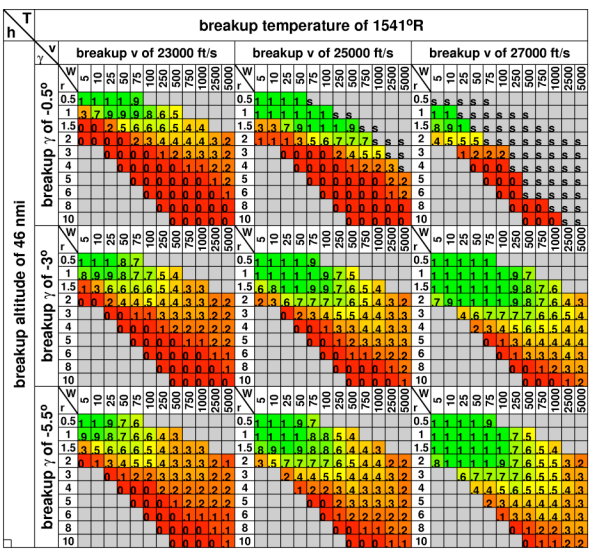

Figure 3c. Aluminum Tumbling Hollow Sphere Survivability for Breakup Altitude of 46 nmi and Breakup Temperature of 1541°R

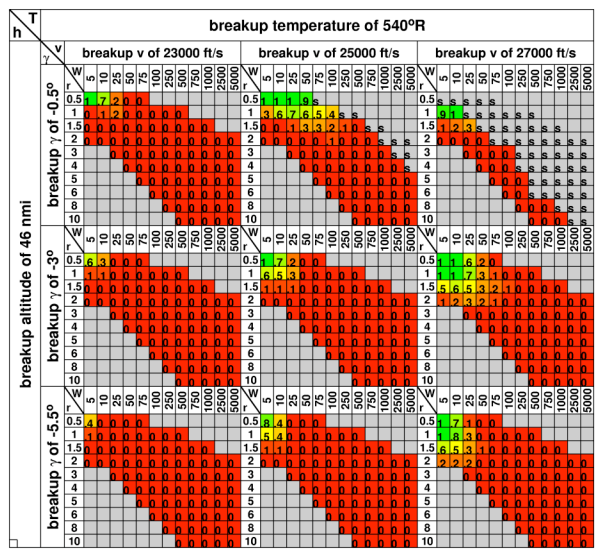

Figure 3d. Aluminum Tumbling Hollow Sphere Survivability for Breakup Altitude of 46 nmi and Breakup Temperature of 540°R

Liquid fraction values

0	.1	.2	.3	.4	.5	.6	.7	.8	.9	1

s Symbol if trajectory skips out of atmosphere (geocentric Earth relative flight path increases to greater than 0°)

Symbol if total mass is greater than mass that could fit inside the sphere or if wall thickness (assuming evenly distributed material along wall) is less than 0.01% of diameter

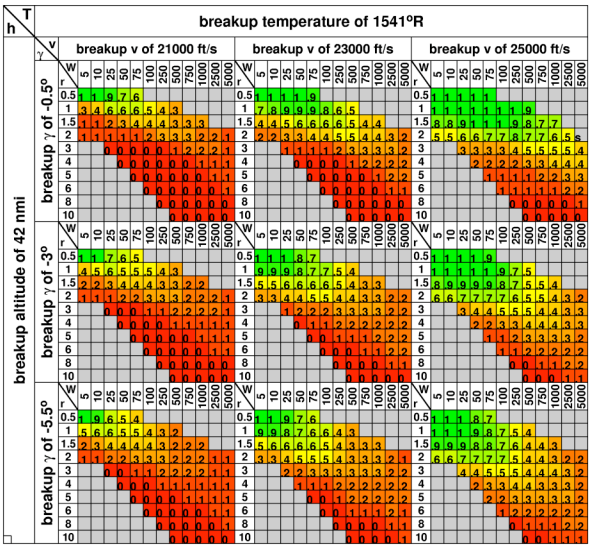

Figure 3e. Aluminum Tumbling Hollow Sphere Survivability for Breakup Altitude of 42 nmi and Breakup Temperature of 1541°R

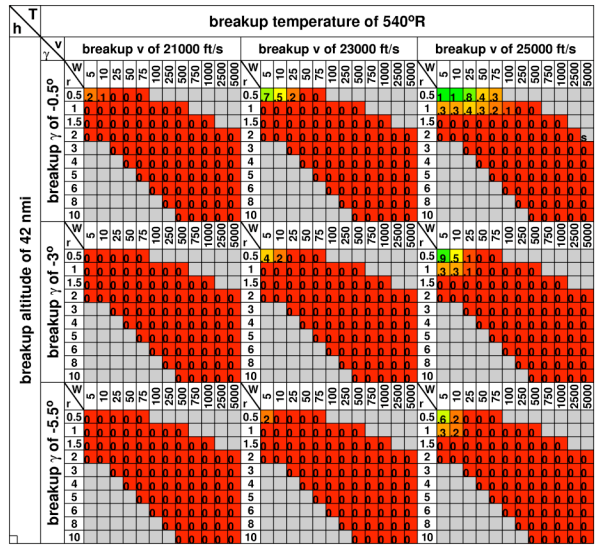

Figure 3f. Aluminum Tumbling Hollow Sphere Survivability for Breakup Altitude of 42 nmi and Breakup Temperature of 540°R

E. Total Casualty Area

Based on all of the analysis above, the total surviving sheltered casualty area of all reentering debris (A_{tsci}) for the ith breakup point is obtained from Eq. (6) by summing the casualty area of each dth piece of debris in the debris model for the ith breakup point.

$$A_{tsc_i} = \sum_d A_{sc_{di}} \tag{6}$$

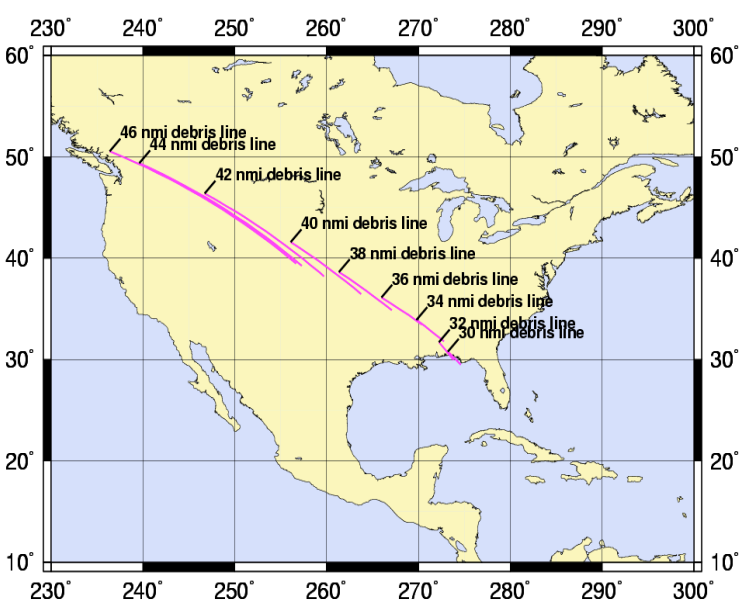

Figure 4. Illustration of Debris Lines for Breakup Points from 30 to 46 nmi

IV. Impact Probability

Given a single i^{th} breakup point, the probability of impact (PI_{ij}) represents the probability that the total sheltered casualty area computed in Section III will impact in the jth area. If the jth area can be modeled as a quadrangle with downrange (dr) and crossrange (cr) dimension, and the jth area is much greater than the size of the total sheltered casualty area, then the probability of impact can be represented by Eq. (7).

$$PI_{ij} = Pf_i \iint f_i(dr,cr)\partial dr \partial cr \tag{7}$$

Where Pf_i is the probability of a catastrophic failure leading to a breakup, and $f_i(dr,cr)$ is the impact probability density function of the ith breakup point for all of the debris included in the total casualty area. Models for the computation of the failure probability and probability density function are discussed below.

Two methods are introduced for

computing the failure probability for these breakup points. Calculation of the total casualty expectation depends on which method is used to compute the failure probability. This is further discussed in Section VI. The first method assumes a failure probability of one for each discrete breakup point. This method is conservative because it assumes that a failure will occur. The second, less conservative method, assigns a different failure probability to each breakup altitude. This is based on Eq. (8), where the failure probability for the entire phase of flight is combined with the dwell time of a single breakup point:

$$Pf_i = Pf_p\left(\frac{t_{i-1} - t_i}{\Delta t_p}\right), \tag{8}$$

where Pf_i is the failure probability for the ith discretized breakup point, Pf_p is the failure probability for the pth phase of flight, Δt_p is the total dwell time for the pth phase of flight, and t_i is the trajectory time at the ith discretized breakup point.

A probability density function is chosen that is uniform in the downrange direction and normal in the crossrange direction. The length of the uniform downrange distribution for a particular breakup point is determined by the debris line. The debris line is a line connecting the low ballistic coefficient debris and high ballistic coefficient debris impact points. These impact points are determined by propagating the lowest and highest ballistic coefficient debris in the debris model to the ground using the aerodynamic properties in Table 1. An example of debris lines for varying breakup altitudes is illustrated in Fig. 4.

The crossrange distribution is represented by a normal distribution centered along the debris line. To determine the crossrange standard deviation, analysis should be done based on vehicle and debris state uncertainty, winds, lift-to-drag ratio, atmosphere, guidance & control, and other unknowns. There is no conservative solution for the crossrange standard deviation; depending on how the population lies, a large standard deviation could make the final result bigger or smaller.

Based on the distributions chosen, the mathematical expression for the probability of the total casualty area from the ith breakup point impacting the jth area is

$$PI_{ij} = \frac{Pf_i \Delta dr_j}{DR_i} \int_{cr_{A_j} - \Delta cr_j/2}^{cr_{A_j} + \Delta cr_j/2} \frac{1}{\sigma_{cr_i}\sqrt{2\pi}} e^{-\left(cr_{A_j}^2 / 2\sigma_{cr_i}^2\right)} \partial cr, \tag{9}$$

where DR_i is the downrange length of the debris line for the ith breakup point, Δdr_j is the downrange length of the jth area (this must be entirely contained within DR_i), cr_{Aj} is the crossrange distance to the center of the jth area, and Δcr_j is the crossrange width of the jth area. Some of these variables are calculated based on the population data introduced in the next section. An illustration of the distribution is shown in Fig. 6 along with a close-up of the distribution shown in Fig. 7.

V. Population Data

Population data is obtained from the Center for International Earth Science Information Network at Columbia University[10]. The population data is in centroidal format. This means population is represented by longitude and latitude along with the population count (P) and area (A) of the centroid. These population centers are shown in Fig. 7. This is different than databases available in gridded format, which represent a fixed geographic size and a population count. Data from this database is input to Eq. (9). The variable cr_A in Eq. (9) is the crossrange distance to the population centroid center. Δcr and Δdr in Eq. (9) are calculated by

$$\Delta dr = \Delta cr = \sqrt{A}. \tag{10}$$

The population density (PD_i) for the jth area is computed using

$$PD_j = P_j / A_j. \tag{11}$$

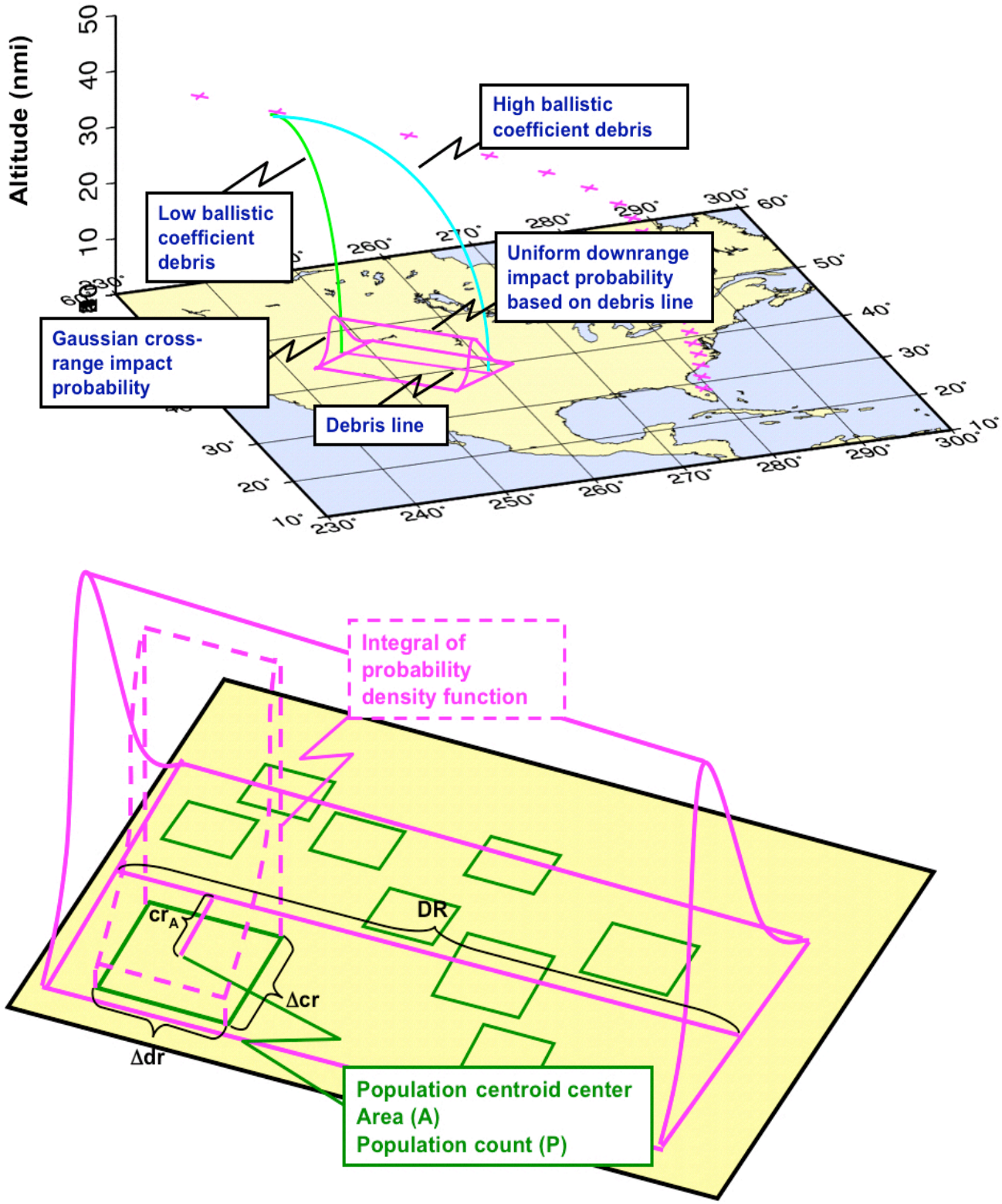

Figure 7. Close-up of Impact Probability Density Function

VI. Casualty Expectation Calculation

Once the breakup point, total sheltered casualty area, impact probability, and population density have been established, the casualty expectation for a single i^{th} breakup point can be obtained from

$$E_{c_i} = \sum_j PD_j A_{tsc} PI_{ij}. \tag{12}$$

Fig. 8 shows an example calculation for a 42 nmi breakup where each dot represents a jth area in Eq. (12). By summing all of the values represented by the colored dots the E_{ci} for a single breakup point is obtained.

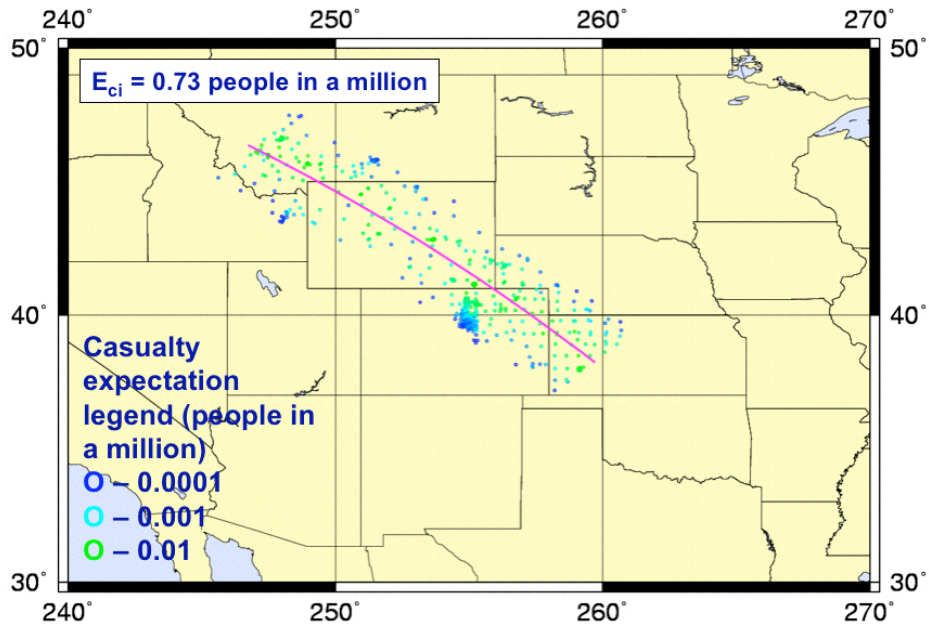

Figure 8. Casualty Expectation for a 42 nmi Breakup

The set of methods developed in Sections III, IV, and V are repeated for each breakup point. Depending on the failure probability method chosen in Section IV, a summation or a maximum casualty expectation is computed from the resulting array of casualty expectations. If a failure probability of one is used for each breakup point, then the maximum casualty expectation from the array of breakup points is taken as the total casualty expectation. If a time based failure probability is used, a summation of casualty expectation is computed. One last check should be made to ensure large changes are not occurring between consecutive breakup points. Areas where there are large changes in casualty expectation should be investigated further by increasing the number of breakup points.

VII. Conclusion

This paper presents a simplified approach for estimating the hazard associated with reentry and breakup of space hardware from low Earth orbit. The method allows the user to make some simplifying assumptions and to develop conservative estimates of the casualty expectation without conducting extensive analyses. The approach also helps a user better understand the various components of a reentry breakup analysis.

Acknowledgments

The authors would like to thank the Federal Aviation Administration for funding this work.

References

[1]Patera, R.P., and Ailor, W.H., "Realities of Reentry Disposal," *Advances in Astronautical Science*, Vol. 99, 1998.

[2]Dobarco-Otero1, J., Smith, R.N., Marichalar, J. J., Opiela, J. N., *Upgrades to Object Reentry Survival Analysis Tool (ORSAT) for Spacecraft and Launch Vehicle Upper Stage.*

[3]*Columbia Accident Investigation Board Report*

[4]Refling, O., Stern, R., and Potz, C., *Review of Orbital Reentry Risk Predictions*, The Aerospace Corporation ATR-92(2835)-1, July 15, 1992.

[5]Cropp, L. O., *Analytical Methods Used in Predicting the Re-Entry Ablation of Spherical and Cylindrical Bodies,* Sandia Corporation, September 1965.

[6]*Casualty Areas from Impacting Inert Debris for People in the Open*, Research Triangle Institute*,* RTI Report No. RTI/5180/60-31F, April 13, 1995.

[7]*Expected Casualty Calculations for Commercial Space Launch and Reentry Missions*, FAA Advisory Circular AC 431.35-1, August 30, 2000.

[8]Detra, R. W., Kemp, N.H., Riddell, F. R., *Addendum to Heat Transfer to Satellite Vehicle Re-entering the Atmosphere,* Jet Propulsion Laboratory, December 1957.

[9]*NASA Safety Standard: Guidelines and Assessment Procedures for Limiting Orbital Debris,* NASA Document NSS 1740. 14, August 1995.

[10]Center for International Earth Science Information Network (CIESIN), Columbia University; International Food Policy Research Institute (IFPRI); and World Resources Institute (WRI) 2000. Gridded Population of the World (GPW), Version 4. Palisades, NY: CIESIN, Columbia University. URL http://sedac.ciesin.columbia.edu/plue/gpw.